# Model and Computer Simulations of the Motion of DNA Molecules during Pulse Field Gel Electrophoresis†

Steven B. Smith,*,‡ Christoph Heller,§,∥ and Carlos Bustamante‡

*Institute of Molecular Biology, University of Oregon, Eugene, Oregon 97403, and Fakultät für Biologie, Universität Konstanz, Konstanz, FRG*

*Received September 18, 1990; Revised Manuscript Received February 19, 1991*

ABSTRACT: A model is presented for the motion of individual molecules of DNA undergoing pulse field gel electrophoresis (PFGE). The molecule is represented by a chain of charged beads connected by entropic springs, and the gel is represented by a segmented tube surrounding the beads. This model differs from earlier reptation/tube models in that the tube is allowed to leak in certain places and the chain can double over and flow out of the side of the tube in kinks. It is found that these kinks often lead to the formation of U shapes, which are a major source of retardation in PFGE. The results of computer simulations using this model are compared with real DNA experimental results for the following cases: steady field motion as seen in fluorescence microscopy, mobility in steady fields, mobility in transverse field alternation gel electrophoresis (TFAGE), mobility in field inversion gel electrophoresis (FIGE), and linear dichroism (LD) of DNA in agarose gels during PFGE. Good agreement between the simulations and the experimental results is obtained.

Pulse field gel electrophoresis (PFGE) is a widely used method for separating large DNA molecules by size. Two different types of PFGE are commonly used. The first type has evolved from the original invention (Schwartz & Cantor, 1984) and now uses homogeneous (nondivergent) electric fields that are periodically tacked through some obtuse angle with equal pulse times and field strengths. This field geometry and switching can be produced in a variety of ways. Here we use the acronym TFAGE (transverse field alternation gel electrophoresis) [as per Olson (1989)] to denote their common field geometry and timing. The second common method, field inversion gel electrophoresis (FIGE) (Carle et al., 1986), involves periodic 180° reversals of the electric field with unequal forward/reverse pulse times or electric field strengths. The two methods, TFAGE and FIGE, employ similar pulse times and field strengths to separate molecules within similar size ranges. A good model of DNA motion through gels should therefore explain the features of both types of separations.

Individual stained molecules of DNA undergoing PFGE have recently been visualized by fluorescence microscopy (Smith et al., 1989; Schwartz & Koval, 1989; Gurrieri et al., 1990). This work has added considerably to our understanding of DNA motion, but miroscope methods alone have not solved the riddles of PFGE because of the following limitations: (1) the objective lenses required for this application have a shallow depth of focus (<1 μm) and often show only a slice of the larger molecules of interest, (2) it is difficult to track a particular molecule for a long time under the microscope, and (3) it is difficult to maintain homogeneous gel and field conditions on a microgel that are comparable to conditions inside a lab-scale gel. With a model and computer simulation it has been possible to mimic the local motions seen in the microscope but also to extrapolate the process through simulated space and time until subtle differences in the molecular motions developed into size separation features similar to those obtained in PFGE.

The two most popular methods for representing DNA macromolecular motion through a gel have been the reptation tube models (deGennes, 1971; Lerman & Frisch, 1982; Lumpkin & Zimm, 1982; Slater & Noolandi, 1985) and the obstruction models (Olvera de la Cruz et al., 1986, 1990; Deutsch, 1988, 1989). Tube models represent the gel as an impenetrable tube that surrounds the DNA, while obstruction models represent the gel as an open array of obstructions that locally exclude the molecule. The obstruction models are more realistic because they give DNA the freedom to bunch up between obstructions and enter the gel sideways in loops or kinks. A supercomputer is required for an obstruction model simulation because of the fine scale (about one persistence length) and because the molecule is prevented from crossing any obstruction by rejecting those moves (iterations) in which the molecule does cross. We present here a *modified reptation tube model* in which the molecule can bunch up inside the tube or leak out the side in kinks. Our model operates on a coarse scale (1 μm) and utilizes all of its iterations so that useful simulations of molecular mobility during PFGE may be run overnight on a personal computer.

## Properties of DNA in Agarose

Certain properties of DNA undergoing gel electrophoresis are evident from fluorescence microscope examination. These properties have been modeled and used in the computer simulation. Since the properties of DNA in free solution are easier to observe and describe, we shall start with this case and extend the description to the case where a gel is present.

Entropic elasticity of individual DNA molecules that are free in solution is evident in microscope observations (Yanagida et al., 1983). It is due to the preponderance of accessible states that are associated with shorter end-to-end distances. The molecule samples these states as the Brownian motion forces of the solvent randomize the directions of submicroscopic straight sections in the polymer. To describe its elastic

† Support provided by Human Genome Center at LBL, Contract DE-AC03-76SF00098, OHER Office of Energy Research DOE, NSF Grant DIR-8820732, and NIH Grant GM-32543 to C.B. Support was provided to C.H. from a European Community Grant BAP 0135-D to F. M. Pohl.

* Corresponding author.
‡ University of Oregon.
§ Universität Konstanz.
∥ Present address: Imperial Cancer Research Fund, Lincoln's Inn Fields, London WC2A 3PX, U.K.

0006-2960/91/0430-5264$02.50/0 

properties, the molecule is modeled as a freely jointed chain, that is, a chain of statistically independent straight sections where the length of each section is one Kuhn length (= two persistence lengths). The mean extension of a molecule subjected to a dimensionless tension $a$ is then given (Bueche, 1962) by the Langevin function $L(a)$:

$$s = \frac{e^a + e^{-a}}{e^a - e^{-a}} - \frac{1}{a} = L(a) \quad (1)$$

where $s$ is the mean fractional extension of the molecule or the end-to-end distance divided by the contour length and $a = b\tau/kT$, where $\tau$ is the tension or force pulling the ends of the molecule apart, $b$ is the Kuhn length of the DNA, and $kT$ is Boltzmann's constant times the absolute temperature.

The force on a DNA molecule due to an external field can be estimated by using an effective linear charge density that is reduced from the formal charge of DNA (one electron per phosphate) by the condensation of counterions (Manning, 1978) and by hydrodynamic interactions with counterions in solution. Measurements of the equilibrium extensions of anchored DNA molecules at various electric field strengths and comparison with eq 1 allow estimation of the electrical force on individual DNA molecules. An effective charge of only 5% of the formal charge was thus determined (Smith & Bendich, 1990). Despite this small effective charge, if a macromolecule is anchored at one end, an externally applied electric field of a few volts per centimeter can easily overcome the entropic elasticity and extend the molecule. For a given point in the molecule, the local tension is caused by the sum of all the effective charges from that point outward to the free end of the molecule, just as the tension in a vertically hanging rope, due to its own weight, varies with position along the rope and equals the weight of the rope below the point of measurement. Sections of the molecule will be extended most near the anchor and contracted like a random coil near the free end. If one considers the molecule as being divided into two sections, that part near the anchor where the local fractional extension, $s$, is greater than 0.5 and that part near the end where $s$ is less than 0.5, then it can be shown, by using eq 1 and assuming a Kuhn length of 0.1 $\mu$m, that the "stretched" part of the molecule extends to within 42 kilobase pairs (kbp)/$E$ of the end of the molecule, where $E$ is the electric field strength in volts per centimeter. For a 5 V/cm field strength, any long anchored DNA molecule is pulled out into the "stretched" state except for 8 kbp near the free end.

The above description applies to molecules in free solution, but a surrounding gel complicates the situation. Microscope observations show that individual DNA molecules inside a gel display an elastic behavior, extending from both ends at once or contracting into the center from both ends at once (Smith et al., 1989). Evidently there is room inside many of the agarose pores (comprising a path several micrometers long) for the local straight sections (persistence lengths) to turn sideways. Microscope observations of phage T2 DNA molecules (164 kbp) in 20 V/cm electric fields indicate that the maximum end-to-end length for these molecules in 1% agarose is about 60% of their contour length (S. Gurrieri, personal communication). The same field strength in free solution would stretch anchored T2 molecules to 96% of their contour length. Apparently a molecule may become taut in the high field but cannot extend completely because gel fibers constrain it to a submicroscopic zigzag path. Besides this reduced maximum stretch effect, there is also a temporary minimum stretch for a polymer previously extended in a gel. If a molecule that has been stretched inside a gel is released from the stretching force, it will rapidly contract (over several seconds) by shriveling up inside pores it already occupies. It will stop short of contracting into a compact random coil, however, and retain some elongation in the original direction. Brownian motion will eventually (minutes to hours) move the molecule out of its aligned set of pores and into a set that comprises a random coil, but on the time scale of a PFGE pulse, there exists a minimum value for $s$ greater than zero. Best PFGE mobility results have been obtained in the simulations when the minimum value of $s$ was set at 12% of the contour length.

It is observed that the leading ends of molecules appear brighter as though they contained an excess of DNA and that the tail end of a molecule, on slipping off an obstruction or U shape, rapidly catches up with the head (see Figure 2). This effect is partially explained by the elasticity of the molecule, but especially for molecules longer than 50 kbp, the primary mechanism for collapse in a constant electric field is a reduced mobility for the head of a molecule as compared with the body or tail. Several factors contribute to this difference in mobility. The head is relatively unstretched by the electric field with the leading 42 kbp/$E$ of it assuming a globular shape (locally $s < 0.5$). The body of the molecule is usually stretched because the trailing end is (or has been) wrapped around some gel obstruction. The head tries to thread several pores at once. The body of the molecule, since it is stretched and threaded through pores that are substantially aligned with the electric field, will proceed with a velocity that nearly equals the bulk electrophoresis velocity, i.e., the velocity the molecule would have if no gel were present. The velocity of the head, however, corresponds to the sieving-limited mobility of the globular section at the leading end.

It has been observed that the area near the head of a molecule undergoing gel electrophoresis often has a forked appearance as the molecule doubles up inside of pores and enters in kinks (Smith et al., 1989). During microscope observations of molecular reorientation during TFAGE (Gurrieri et al., 1990), it was observed that a highly stretched molecule would not form kinks when the electric field direction was switched 90°, but if the molecule was first allowed to relax to its minimum stretch ($s = 0.12$) by turning off all fields, then kinks rapidly formed in the new direction when the new field was applied.

## Physical Model

Our model is based on the reptation tube model insofar as the DNA polyion is represented as a string of charged beads and the gel is represented by a smooth segmented tube surrounding the string. In this model, each bead represents 10 kbp of DNA (34 Kuhn lengths) and each tube segment is 1 $\mu$m in length. The beads are separated by entropic springs, which can extend or collapse in response to the forces on the beads. Unlike early reptation models, these beads are not spaced at a constant distance inside the reptation tube but are arranged by forces somewhere between a minimum and maximum separation.

The beads are moved through the tube by three forces (electrical, Brownian, and interbead elastic) and retarded by a viscous drag from the liquid that fills the tube. The equation of motion for a bead is the Langevin equation, in which the mass and acceleration of a bead are neglected and such a velocity is instantly attained where the drag force balances the sum of the drive forces:

$$dx/dt = \text{sum-of-forces/visc-drag-coeff} \quad (2)$$

Here $x$ is the distance along the contour of the tube. The electrical force component is the effective electric charge on

the bead times the scalar product of the electric field vector with the local tube segment direction (unit) vector. The Brownian force is modeled as a uniform deviate random number ranging between plus and minus BrownianForce/$(dt)^{1/2}$. Here "BrownianForce" is a modeling parameter. In order to make this force component scale properly with $dt$, the simulated time per iteration, it must be divided by the half power of $dt$. The interbead elastic force is due to the entropic elasticity of any polymer in solution. To determine the interbead elastic tension $\tau$ from the interbead spacing, the inverse Langevin function is determined from eq 1, namely

$$\tau = (kT/b)L^{-1}(s) \quad (3)$$

An outward-moving end bead, that is, any bead at the end of a chain or subchain that is moving away from the center of the chain, is made to move more slowly than an internal bead experiencing the same force. This simulates the sieving retardation of the unaligned DNA at the leading ends of the polymer. An outward-moving end bead moves at a reduced speed which is some constant fraction (1 - obstructionFactor) of the speed determined from eq 2. All the trailing beads are moved normally by their forces so that the beads inside the chain bunch up against the leading end. They are not allowed to pass or push the end bead but rather the end bead proceeds at its own slower pace, oblivious, so to speak, of the traffic jam behind it.

When an end bead moves outward and leaves the end tube segment, a new tube segment is created to enclose it. Its direction is chosen with a Boltzmann probability distribution such that

$$P(\alpha) = e^{-qEa\cos\alpha/kT} \quad (4)$$

where $P$ is the probability that the tube segment will form an angle $\alpha$ with the electric field direction, $E$ is the electric field strength, $a$ is the length of a tube segment, and $q$ is the effective charge on a single bead.

To simulate kinks, the chain of beads is allowed to divide into subchains that act somewhat independently. Where the beads are condensed to three or more beads per segment (30 kbp/$\mu$m), the chain or subchain is allowed to divided into two subchains which meet at that point. If the independent subchains move together and collide, then a pair of superimposed segments, called "kink segments", are inserted between the subchains. The ends of the subchains are always made even inside the kink by shifting beads from one subchain end to the other as required. If the subchains move into and fill the kink segments, then new kink segments are added and the kink grows. If they pull away from the kink segments, then kink segments are deleted from the end of the kink until the kink disappears. Then the subchains are rejoined as a larger chain. Figure 1 depicts a typical evolution of states as a chain of spring-connected beads moves down a reptation tube.

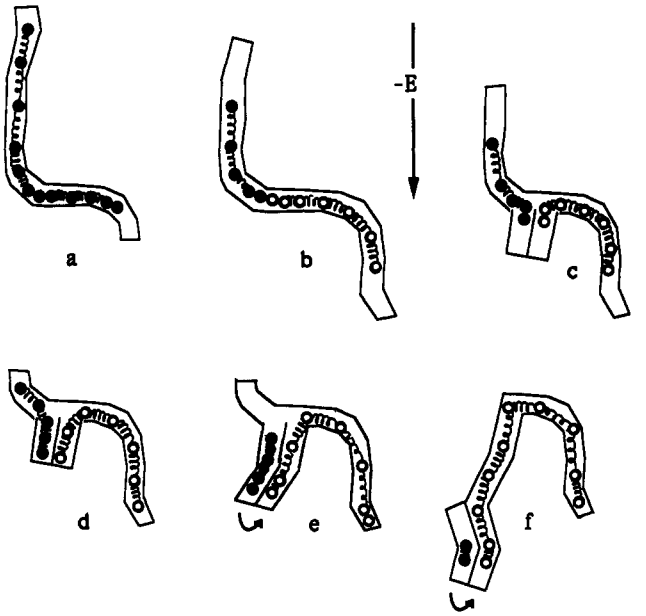


FIGURE 1: Time sequence of bead motion through a segmented tube. The electrical force on the negatively charged beads is downward. Entropic elasticity is indicated by springs. (a) The chain is moving downward but has selected a semirandom path that deviates significantly from vertical. (b) The beads have bunched at the bend and therefore the chain is broken into two subchains. The beads in the second subchain are identified with white centers. (c) The subchains have moved together and the end beads would overlap except that two parallel kink segments are inserted between them. The kink segment pairs are depicted here as adjacent (for clarity) but they are actually superimposed in the computer program. (d) The left subchain flows downfield into the left kink segment while the right subchain stretches its springs to extend from both ends. (e) The kink segments have been extended and the right chain has formed a nearly symmetrical U. One of the left chain's beads has crossed over to the right chain. (f) The kink is further extended with another pair of segments and two more beads have crossed over. In further sequences (not shown) the left chain will completely disappear, leaving the left arm of the inverted U longer than the right arm. The internal springs will become nearly fully extended and the chain will siphon off into the left arm.

## Computer Simulation of the Model

The program is written in Pascal and the molecular motion is accomplished in the following loop:

```
Repeat
    FindForces;
    MoveBeads;
    AdjustTube;
    CreateKinks;
until EndOfRun;
```

These procedures are approximations of the physical model (above). Assumptions in the procedures that modify the physics of the model are described below. Those sections of the procedures that are substantially in agreement with the physical model are not described.

*Find-Forces.* For the purposes of computation, the entropic spring tension between beads, as described in eq 3, is approximated as

$$\tau = \text{springForce}(s + s^3 + s^5) \quad (5)$$

where $s$ represents the fractional bead separation (bead separation/maximum separation) and springForce is a modeling parameter. Equation 5 departs no more than ±12% from eq 3 for $0 < s < 0.84$, but the force in eq 3 goes to infinity at $s = 1$, a fatal error during a computer simulation. An inelastic collision at maximum bead spacing, described below, substitutes for an impenetrable barrier at this extreme without bouncing the bead back an infinite distance on the next iteration. For low fractional elongation, eq 3 can be approximated by $\tau = s(3kT/b)$. Assuming $b = 0.1$ $\mu$m, the term $3kT/b$ equals 0.75 eV/$\mu$m, which would normally be the springForce used in eq 5. However, the maximum bead spacing is less than the contour length (3.4 $\mu$m) because of the submicroscopic zigzag path through the gel. Therefore, when the beads are spaced by the maximum bead spacing, the Kuhn-length links are locally entirely aligned with the submicroscopic straight sections between the gel obstructions. The fractional elongation $s$ is therefore defined (in the program) as the local bead spacing divided by the maximum bead spacing (2 $\mu$m). By this new definition of $s$, eq 3 gives the tension in submicroscopic straight sections of the chain, which

are at an angle from the direction of the reptation tube segment such that the average cosine of that angle is (2/3.4). Therefore, the constant in eq 5 is corrected for this indirection of forces by making springForce = $(2/3.4)3kT/b$ = 0.44 eV/$\mu$m.

The electrical force on a bead equals the projection of the external electrical field along the local tube direction multiplied by the bead's effective charge.

The magnitude of the Brownian force component was chosen to make the simulation look most like microscope observations, that is, it duplicates a slight motion within the gel that is visible in the microscope. Without any Brownian or electrical forces in the simulation, a chain of beads would contract to its minimum length and remain motionless forever. With Brownian forces, the chain does what real molecules do; namely, it reorients eventually into a different set of pores. The Brownian forces are made proportional to a modeling parameter BrownianForce and scaled by division with the square root of d$t$, the time per iteration. Then for each bead on each iteration, this constant is multiplied by a uniform deviate random number between −0.5 and +0.5.

*Move-Beads.* During each iteration of the program, which represents a simulated time increment d$t$, each bead is moved along the reptation tube by the Pascal equivalent of eq 2:

```
positionOfBead[i] :=
    positionOfBead[i]+forceOnBead[i]*dt/viscDragCoeff;
                                                    (6)
```

If the iteration time is made too long, a slight displacement of a bead from its equilibrium spring position between its neighbor beads will cause an elastic restoring force, which, when carried through the next iteration, will place the bead even farther off center in the opposite direction. Successive iterations will then build up an exponentially increasing magnitude of oscillation and the simulation is said to have a numerical instability or parasitic oscillation. These problems have been dealt with by making the time d$t$ small (usually 0.05 s) and by using a sort of inelastic collision to limit the motion of the beads. The interbead spacing is constrained to fall between a minimum (0.4 $\mu$m) and a maximum (2.0 $\mu$m). After an application of eq 6, the center of mass (along the tube) of the chain is calculated. Then the bead spacing is corrected, starting at the biggest gap, to be no larger than the maximum 2.0 $\mu$m. The spacing is again corrected, starting at the most condensed spot, to be no less than the minimum allowed space (0.4 $\mu$m). The whole chain is then shifted laterally to give the same center of mass as before the spacing changes.

In our program, all processes of motion are determined by eq 6 and so all mobilities are inversely proportional to the viscous drag coefficient. Therefore, the drag coefficient is a convenient place to compensate for changes in temperature or gel concentration, insofar as these factors affect the mobility of DNA molecules in a gel. In the program, there is a constant "specific drag coefficient" (SDC), which is so named because it specifies the drag at at 20 °C in 1% SeaKem ME agarose (0.5× TBE). For arbitrary conditions, the viscous drag coefficient used in eq 6 is given by

$$\text{viscDragCoeff} := \text{SDC}*\frac{3}{5-2*\text{agarosePercent}}*\frac{2}{1+0.05*\text{temperature}} \quad (7)$$

This formula was created empirically to reproduce, to linear approximation, the variation of electrophoretic mobility with temperature and agarose concentration for very long DNAs (>50 kbp) in high fields (~5 V/cm). The value of the specific drag coefficient was chosen arbitrarily but the value so chosen, 0.05 eV s/$\mu$m$^2$, when applied directly (without obstruction factor or kinking) to a bead with 1000 electrons effective charge, gives the same mobility as in bulk electrophoresis experiments, i.e., 2 ($\mu$m/s)/(V/cm) (Olivera et al., 1964).

The retardation of the bead motion at the nascent end of a reptation tube is accomplished by use of the "obstructionFactor", whereby the end bead in a chain is not alway moved by eq 6 but is left stationary for a certain fraction of the iterations as though it were undergoing a collision with the gel. An obstructionFactor of 0.7 would mean that, for each iteration, if an end bead has a force moving it outward, there is a 70% probability (realized with a random number generator) that the end bead will be frozen in position. The end bead may be frozen anywhere inside its tube segment, not only at the edge where it is about to exit and form a new segment.

*Adjust-Tube.* As in previous biased reptation models, when a bead exits one of the ends of the reptation tube, the tube is extended by a new segment. When the end bead retracts inside the tube leaving the end segment empty, that segment is deleted. The representation of the gel exists only locally around the bead chain. The direction for a new segment is chosen by a random number generator with a biased probability as described by eq 4 with $a$ = 1 $\mu$m and $q$ = 1000 e. Once the beads have retracted into a tube past the end segment, that segment is deleted from the array of segments in use.

*Create-Kinks.* To determine where bunching occurs, the beads are counted in each of the tube segments along a chain or subchain. If the concentration of beads is three or more per segment, then the chain is broken at that spot and two subchains are formed. The two adjacent end beads are no longer strictly subject to the minimum and maximum spacing rule, which only applies within a subchain. If, on the next iteration, the forces cause the subchains to move together so that the end beads overlap, then two antiparallel superimposed tube segments (called kink segments) are created, with their common direction chosen according to eq 4. One kink segment is attached to the first subtube, becoming the last segment in that subtube. The other kink segment is attached to the second subtube and becomes its first segment. With time, the adjacent subchains will siphon into or out of this pair of kink segments, depending on the forces applied to these subchains and subject to the retardation of an outward advancing end bead (obstructionFactor). As the subchains move, the lengths of the subchains are made even in the MoveBeads procedure so the two subchains drape evenly inside the kink. If, after evening off the ends, the subchains are dangling past the ends of the kink segments, then the kink is extended with another pair of superimposed segments. If the forces are such that the subchains pull all the beads out of a kink, then the two subchains are rejoined at the location of the former kink into one long chain (or subchain).

*Modeling Parameters.* This model contains several adjustable parameters (fudge factors), which attempt to describe DNA, agarose, and buffer and which are given here in units of microns, seconds, electronic charges, and volts. One bead is assumed to equal 10 kbp of DNA.

d$t$ = 0.05 s (typical)
maxBeadSpace = 2.0 $\mu$m
minBeadSpace = 0.4 $\mu$m
springForce = 0.44 eV/$\mu$m
$q$ = 1000 electronic charges/bead
specDragCoeff = 0.05 eV s/$\mu$m$^2$
brownianForce = 0.025 eV (s)$^{1/2}$/$\mu$m

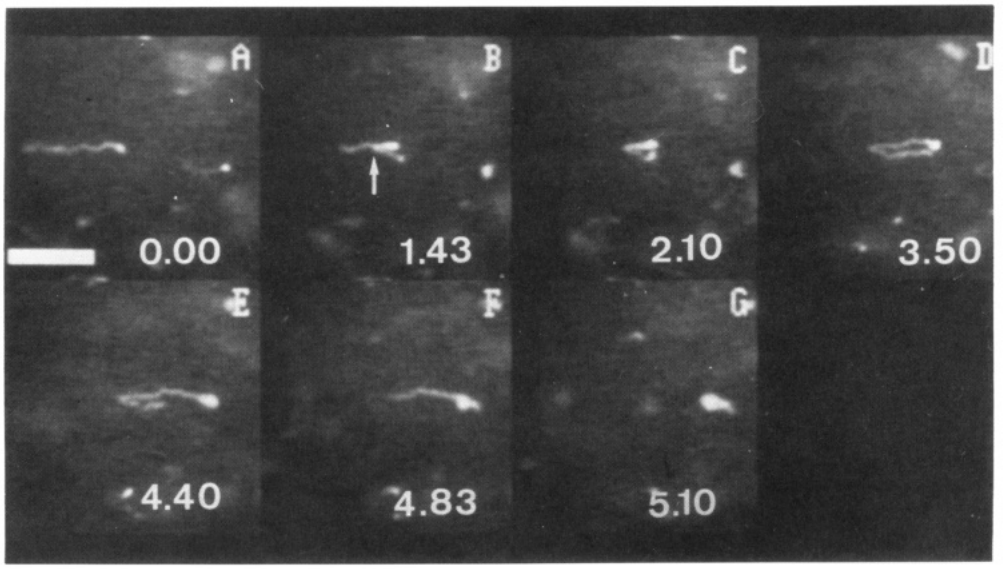


FIGURE 2: Time sequence of T2 phage DNA molecule, stained with acridine orange, moving through 1% agarose (Gurrieri et al., 1990). Electrical force is toward the right. Numbers indicate time in seconds. The arrow in frame B indicates where a kink starts forming on top of the molecule. Field strength equals 10 V/cm. Scale bar equals 8 $\mu$m.

obstructionFactor = 0.7

The value of these parameters remained fixed for all the simulations which produced the following results.

## RESULTS

*Comparison with Microscope Observations.* Figure 2 shows a time sequence of DNA motion (Gurrieri et al., 1990) with an image-intensified television camera coupled to a fluorescence microscope. In Figure 3 there is a two-dimensional projection of the molecular motion simulation, also shown as a time sequence. Note that in both figures the molecules move in a cyclic fashion of stretching and condensation. When a molecule is stretched straight and aligned with the field, its tail starts catching up with the head. When some region of a molecule has condensed, with the collapse beginning at the leading end, kinks grow out of the condensed area. The material that had been in the tail then flows into the kink while the head of the molecule grows by siphoning out of the other side of the kink. When the trailing end of the molecule enters a long kink and falls to the bottom, a J or U shape has been formed. Then the forces are such as to extend the molecule and pull out any internal kinks. The molecule assumes an extended U shape with its apparent length in the microscope greater than half its contour length. The molecule then slips off into the side with the longer arm. The formation of kinks is necessary and sufficient for the formation of U shapes and for the continual cycle of compression and elongation.

*Steady Field Mobilities.* Figure 4A shows the results of a simulation in which chains of different lengths are exposed to steady electric fields, while Figure 4B shows the same experiment conducted on real DNA. In both figures the various species essentially comigrate or fail to resolve by size. This comigration is rather surprising considering that molecules move by continually entering U shapes and slipping off. Longer molecules form longer U shapes, which persist for a longer time, but short molecules (<30 kbp) seldom form U shapes that are visible in the microscope. One explanation for comigration is that the delay from trapping in a U shape is seldom the rate-determining step in the migration of the molecule; rather, the principal source of retardation is sieving of the leading ends. Close examination of Figure 2 illustrates this point. Assume that the bright leading ends of the molecule in Figure 2 have sieving-limited velocities and note that the

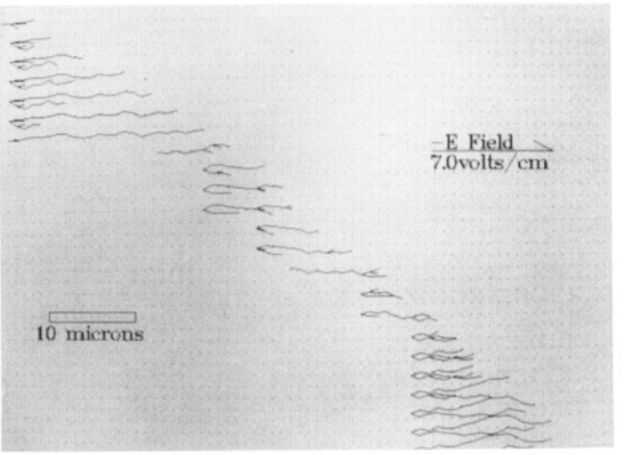


FIGURE 3: Computer simulation of DNA motion. The chain is moving toward the right due to the electric field but is shown offset downward each 1.0 s in order to show the progression of states. The chain consists of 17 beads, which corresponds to the size of T2 phage DNA. Simulated field equals 7 V/cm. Scale bar equals 10 $\mu$m. The array of dots, with 1-$\mu$m spacing, is shown to aid comparison of states. The dots do not represent obstructions in the gel.

molecule is always advancing on at least one front with this velocity. In Figure 3 the motion of the molecule is seen as a diagonal trace and the trailing end of the molecule is seen to move in jumps. Note the left side of the diagonal pattern in Figure 3 is jagged but the right side of the diagonal trace is relatively smooth, indicating that the progress of the leading ends is steady. Only a very symmetrical U shape will delay the progress of the leading ends. The comigration is then due to the fact that very large (>50 kbp) molecules move at the sieving rate of their leading end(s).

*TFAGE Mobilities.* Panels A and C of Figure 5 show the results of a computer simulation of a TFAGE experiment, while panels B and D show the real experimental results of Birren et al. (1988). The simulation reproduces certain features of the real DNA results, namely, (1) the absolute velocities for each size DNA in a given switch time are similar, (2) the mobility curves converge to a common point for small DNAs, (3) the curves do not reach zero mobility for long DNAs but approach a common minimum velocity, and (4) inflection points, i.e., changes in slope, are evident near the

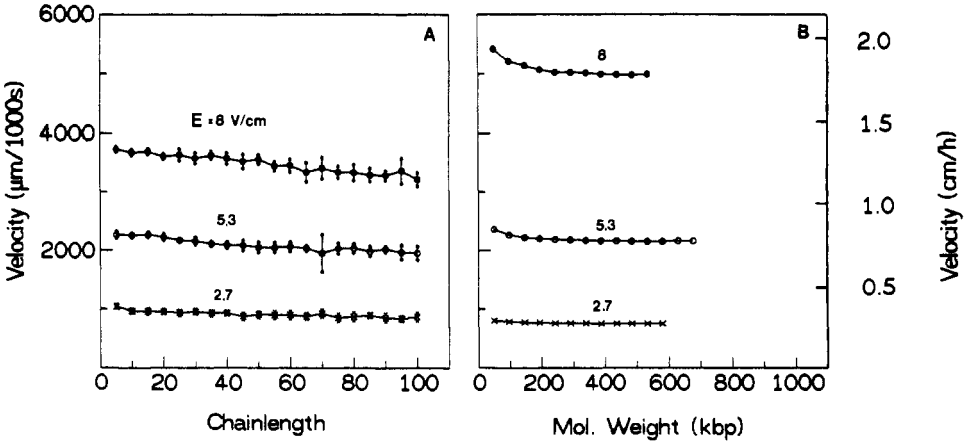


FIGURE 4: (A) Simulated velocities for chains (multimers of 5 beads) with eq 7 evaluated for 1% agarose and 18 °C. Simulated run time was 1000 s. Error bars represent the SD of 13 chains of each size. (B) Velocities of multimers of λ DNA (48.5 kbp) in 1% agarose and 0.5× TBE buffer at 18 °C in three steady fields of different strengths (Heller, 1990).

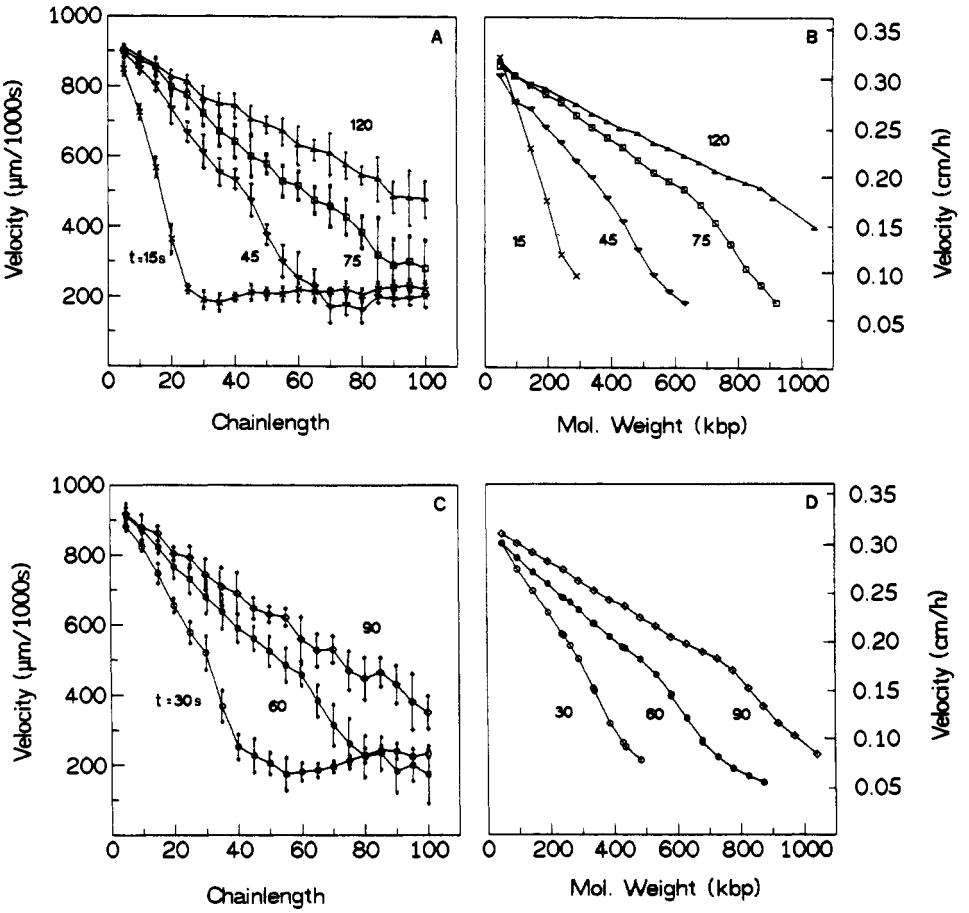


FIGURE 5: (A,C) Simulated velocities for 5-bead multimers in a TFAGE field with 120 °C tack angle, 5 V/cm, and eq 7 evaluated for 1% ME agarose at 13.5 °C. Error bars represent SD in velocities of 12 chains, each run 1000 s. Electric field switch times ($^1/_2$ cycle times) are indicated next to each curve. (B,D) Velocities of λ multimers in a TFAGE field as produced by a PACE apparatus (programmable autonomously controlled electrodes) (Birren et al., 1988). Molecules were run in 1% SeaKem LE agarose and 0.5× TBE buffer at 13.5 °C. Field strength was reported to be 6 V/cm but may actually have been lower than 5 V/cm (see Appendix A).

middles of the real DNA curves for 60-, 75-, and 90-s switch times and near the middles of the simulation curves for 30-, 45-, and 60-s switch times.

To try to understand the separation mechanism at work in TFAGE, the real-time output of the computer simulation was observed while different size chains separated by size in a simulated TFAGE field. Identical chains in an ensemble assumed a confusing variety of shapes as they followed the tacking field. Molecules sometimes formed the chevron shape with 120° included angle characteristic of Southern's switchback model (Southern et al., 1987). Other chains failed to make progress during a tack because they entered a narrow U shape, as in Figure 3, and failed to siphon out of it before the field was reversed. Still other molecules formed broad-base U shapes slanted in the new field direction, where the leading arm made a 120° angle with the base and the trailing arm made a 60° angle with the base. Here the leading arm usually won after some delay. The size separation in TFAGE appeared to occur mainly when the molecules assumed shapes similar to Southern's model. Just as with real DNA, the size separation in the simulation was nearly lost when the tack angle of the electric field was reduced from 120° to 90°.

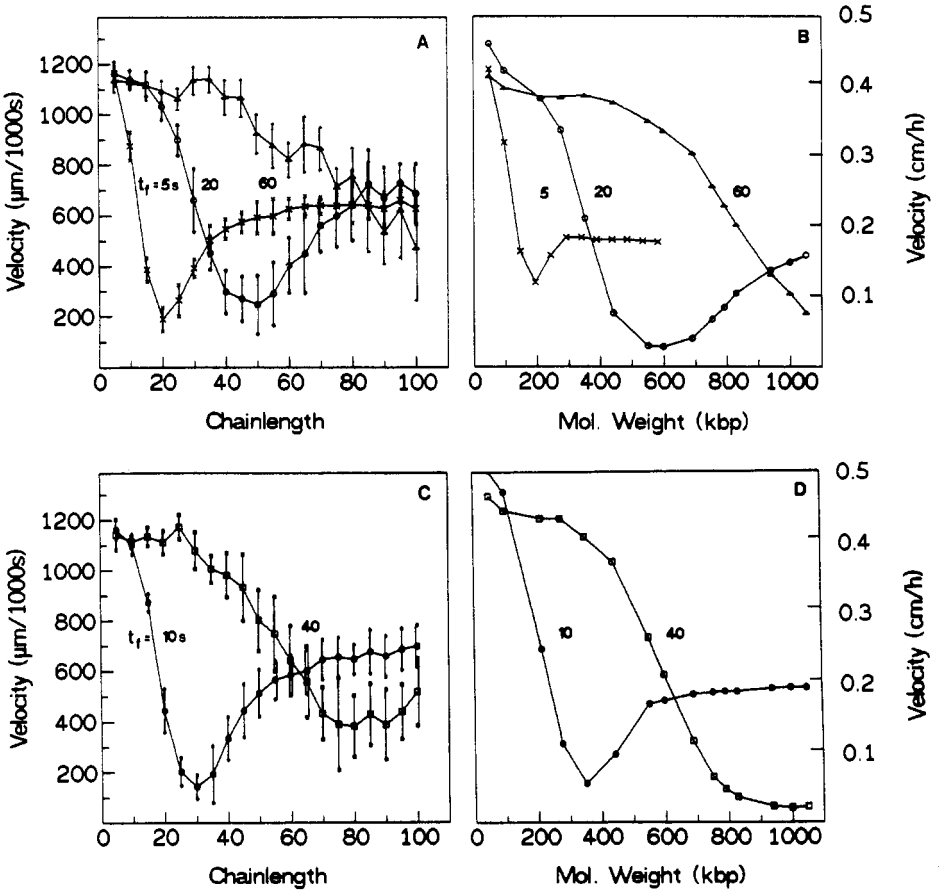


FIGURE 6: (A,C) Simulated velocities for 5-bead multimers in a FIGE field of 5.3 V/cm with eq 7 evaluated for 1% agarose at 18 °C. The curves are labeled with the forward pulse time; the reverse time was one-third of the forward. The error bars represent the SD in the velocities of 20 chains each run for 1000 s. (B,D) Velocities of yeast chromosomes in a FIGE field at different pulse times (Heller & Pohl, 1989). Conditions: 5.3 V/cm, 1% agarose (BRL 5510UB) and 0.5× TBE, 18 °C, 3:1 forward:reverse time ratio and run time of 18 h.

*FIGE Mobilities.* Parts A and C of Figure 6 show the simulation results for a FIGE experiment, and panels B and D show the same experimental conditions applied to real DNA (Heller & Pohl, 1989). The mobility minima are present since the pulse times were not ramped but rather held constant with a 3:1 forward:reverse time ratio. The simulation results are similar to the real DNA experimental results in the following ways: (1) the simulation curves have minima that are similar in depth, width, and position to the real DNA curves, (2) the simulation curves converge to a common velocity for small-length chains, as do the real DNA curves, and these absolute velocities are the same, (3) the simulation curves converge to a common velocity for very large chains, as is the case with real DNA, and (4) the pulse time vs size range of maximum FIGE resolution is about the same for simulated and real DNA.

The simulation results differ from the real DNA in two ways: (1) The depths of the mobility minima decrease with pulse time or chain length, while the opposite is true for the real DNA curves; a possible explanation will be discussed below. (2) The simulation curves recover about 30% too much of their velocities on the large-chain side of the mobility minima.

The reason for the mobility dip in FIGE was made evident by watching the real-time simulation graphic output. Those chains that were smaller than the mobility minimum had enough time to form several U shapes and slip off during either the forward or reverse pulse time. Those chains that were at the mobility minimum size were trapped in a recurring U shape. Whatever progress was made in forming a U during the forward pulse was wiped out during the reverse pulse. Although the reverse pulse had one-third the duration of the forward pulse, U shapes retracted much faster than they extended. During extension, the elastic and electrical forces opposed, but during U retraction, the elastic force aided the electrical force. Also during U extension, the outward-moving end beads were retarded by sieving, but during retraction, the pores were already threaded. Chains above the mobility minimum size regained some mobility because the reverse pulse was not long enough to reset the chain to its random coil size. Therefore, some U extension was carried over between forward pulses and the molecule slowly slipped around the bend of the U shape. The arms of a U shape for a very long chain often failed to retract during the reverse pulse because the condensed ends formed reverse U shapes (hooks), which delayed the contraction of the main U shape.

Several other models have successfully duplicated the mobility minimum in FIGE. These models all describe a variable-length (elastic) chain that becomes trapped in a U shape (Deutsch & Madden, 1989; Duke, 1989; Zimm, 1988).

*PFGE Band Resolution.* The error bars shown on the simulation curves (Figures 4A, 5A,C, and 6A,C) represent the rms deviations in the end-point positions of several chains, all of the same size, that were started from identical positions and configurations but with different initial random number seeds. Their end-point distribution is therefore a simulation of the DNA band width, in a real gel, assuming the DNA molecules started from a perfect zero-width well and further assuming that the molecules acted independently (no overloading). Since the end-point distribution is the result of a "random walk", its width scales as the square root of time, whereas the displacement of a band's center scales linearly. The simulation

band widths in the figures may seem large, but they would compare favorably with real gels that were run for only 1000 s. If the computer had run long enough to simulate a 10-h run, then the typical band width for steady field electrophoresis at 5 V/cm would be about 1 mm. This value is in good agreement with experiment for molecules started from a very thin well (data not shown). If our model is accurate, insofar as the progression of states and velocities of a molecule is concerned, then this represents as narrow a band width as will ever be attained for very long DNA reptating by collapse and expansion through 1% agarose. The simulation band widths have some other features in common with real band widths; e.g., they increase with the length of the chains, as with real molecules, and the band widths for FIGE are generally larger than for TFAGE, as in real experiments.

*Linear Dichroism.* Linear dichroism (LD) of DNA undergoing PFGE is a way of looking at the submicroscopic alignment of the molecule as averaged over many molecules at once. It is based on the idea that the transition dipole moment of a DNA base or of an intercalating chromophore is at a fixed angle with respect to the local longitudinal axis of the molecule. Since this angle is close to 90°, it can be shown for a straight section of DNA polymer that the amount of absorption of linearly polarized light is nearly proportional to $\sin^2\theta$, where $\theta$ is the angle between the electric field of the light and the long axis of the DNA. Dichroism experiments performed on DNA in agarose gels have involved measuring the absorption of light that was linearly polarized parallel to the electrophoretic field direction ($A_\parallel$) and also the absorption of light polarized along some axis perpendicular to that direction ($A_\perp$). The "reduced linear dichroism" is defined as $(A_\parallel - A_\perp)/A_{iso}$, where $A_{iso}$ is the absorption from that same DNA which is not aligned by an electrophoretic electric field. We have simulated the dichroism of molecules in various configurations by summing the contributions to $A_\parallel$ and $A_\perp$ from each bead along the chain. The spacing of the beads would indicate the local stretch, and the orientation of the tube segment surrounding a bead would indicate the local direction of that stretch. For the purposes of computing dichroism, the DNA *cannot* be considered as straight between two beads. What is needed to calculate the light absorption is the average of $\sin^2\theta$ along the length of polymer connecting two beads. This quantity can be estimated by using the freely jointed chain model and assuming the DNA is constructed of 0.1-$\mu$m (Kuhn length) segments, which themselves are straight. Each bead therefore represents 34 of these segments strung together. It is further assumed that the separation between adjacent beads is caused by mechanical tension along that section of molecule and that this tension ($\tau$) is constant for the 34 Kuhn segments comprising the bead and is directed along the reptation tube segment surrounding the bead. The Kuhn segments are assumed to lie in a distribution that is biased toward alignment with the tension vector by the Boltzmann factor $e^{-b\tau\cos\phi/KT}$, where $\phi$ is the angle between the Kuhn segment and the tension. It can be shown (see Appendix B) that

$$\langle\sin^2\theta\rangle = \sin^2\alpha\left[1 - \frac{3s}{L^{-1}(s)}\right] + \frac{2s}{L^{-1}(s)} \qquad (8)$$

where $\alpha$ is the angle between the reptation tube segment and the light electric field, $s$ is the local stretch of the molecule redefined here (again) as the local bead spacing divided by 3.4 $\mu$m (the contour length of 10 kbp), and $L^{-1}(s)$ is the inverse Langevin function of $s$. The first term represents the dichroism signal since it depends on the angle $\alpha$, which changes for $A_\parallel$ or $A_\perp$. The factor $[1 - 3s/L^{-1}(s)]$ is a positive even function for $-1 < s < 1$. For computational speed this factor was approximated by $s^{2.7}$, this being a sufficiently good fit since the results (shapes of the curves in Figure 7) are not much affected by using much worse fits, e.g., $s^2$ or $s^3$. In the computer simulation, the reduced linear dichroism for a chain with $N$ beads was computed as

$$\text{reduced LD} = \frac{A_\parallel - A_\perp}{A_{iso}} = \frac{\sum_{i=1}^{N}\sin^2\alpha_{x,i}(s_i)^{2.7} - \sum_{i=1}^{N}\sin^2\alpha_{y,i}(s_i)^{2.7}}{2N/3} \qquad (9)$$

where the denominator, $A_{iso}$, is given by eq 8 when $s = 0$. The angle $\alpha_{x,i}$ is the angle between the reptation tube segment surrounding bead $i$ and the $x$ axis, which is parallel to the electrophoretic field direction. The angle $\alpha_{y,i}$ is the angle between the reptation tube segment and the $y$ axis. The $z$ axis or any direction in the $yz$ plane would have served as well, but just as in the real experiment, some single direction had to be chosen for the $A_\perp$ light beam's polarization.

Figure 7A is a plot of the fluorescence-detected LD from $\lambda$ multimers exposed to PFGE (Holzwarth et al., 1987). Figure 7B is a plot of the simulated reduced LD for 200 chains ranging from 5 beads (50 kbp) to 25 beads (250 kbp). Each of the 200 chains was started as a different random coil and then exposed to four pulses of alternating polarity. The simulated conditions were the same as for the experiment of Figure 7A. The real and simulation LD waveforms have similar shapes. The rise and fall times are comparable and vary in the same way with DNA length.

Figure 7C shows the simulated reduced LD of the same length chains with a single polarity pulse of 9 V/cm applied for 20 s. These conditions are the same as in the experiments of Akerman et al. (1989), except that instead of averaging the LD from many molecules, Figure 7C shows the simulated LD from a single chain. The LD peaks correspond to the extended U or J shape, and the LD minima occur when the chain has slipped off the U and collapsed. These peaks are positioned randomly, dependent on the initial random seed. Figure 7D shows the same conditions as for panel C except that the LD from 200 chains (each with a different seed) was averaged, much as a real LD experiment views an ensemble of molecules. Here the curve is similar to the reults (not shown) of Akerman et al. (1989) in that the LD signal rises to a peak and then falls back to a steady-state value. The states of the 200 chains are well correlated at the start of the electric field pulse because all the chains are initialized as compact random coils. Real DNA macromolecules, which have not been exposed to an electric field for some time (minutes to hours), will likewise assume compact random coil shapes in agarose. The correlation of states persists for some time after the electric pulse begins. Many of the chains reach a U shape at about the same time, and this accounts for the overshoot peak. The lower steady value of LD occurs when temporal correlation is lost between the shapes of the 200 chains and an equilibrium of extended and collapsed shapes is reached. Similar conclusions has been reached by others (Deutsch, 1989; Lim et al., 1990).

## Discussion

This model has reproduced many of the features of microscope observations, PFGE separations, and LD experiments. The physical assumptions of the model, such as elasticity, tube confinement, kink formation, and obstruction factor, are gross generalizations of the atomic-scale interaction between agarose and DNA and, as such, should not be expected to apply very

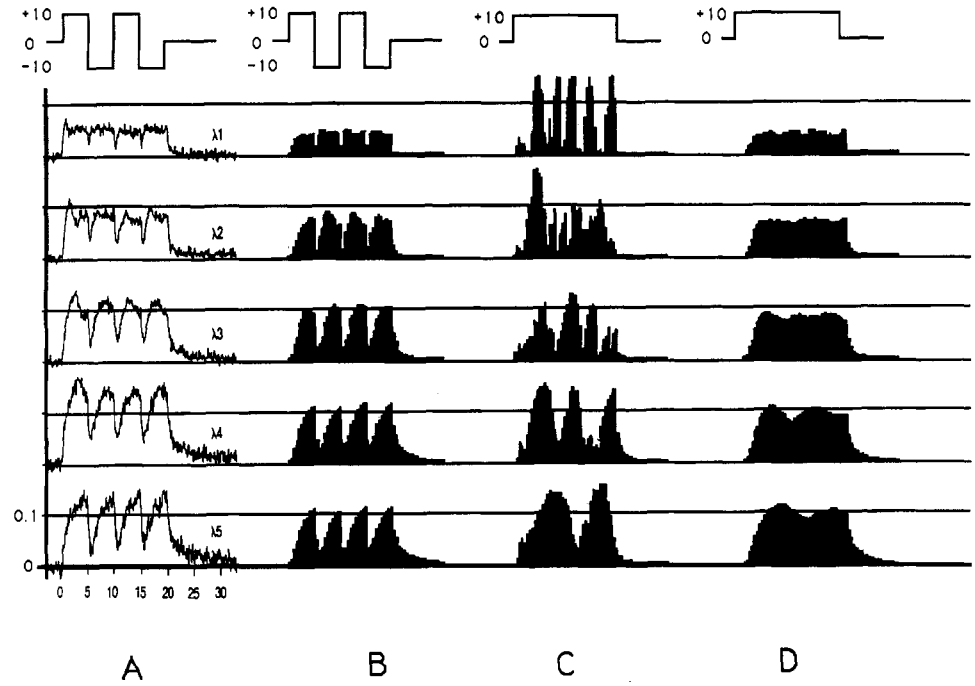


FIGURE 7: (A) Fluorescence-detected linear dichroism orientation function for first five multimers of λ in a pulsed electric field (Holzwarth et al., 1987). The electric field is represented in the top trace and is ±10 V/cm. (B) Simulated reduced LD as computed by eq 9 and averaged over 200 chains. Conditions were the same as in the experiment of panel A. The LD signal for DNA is negative so these plots are inverted. (C) Simulated reduced LD for first five multimers of 5-bead chain with a 20-s "on" pulse at 9 V/cm followed by a 10-s "off" pulse with zero field. One chain of each length was observed. (D) Same conditions as in panel C except 200 chains were observed and averaged in time.

far outside the range of microscope observation or PFGE conditions. Where the generalizations fail, we gain insight into the physics that was overlooked.

The model loses accuracy for molecules that are too short. In Figure 7A, an overshoot is visible at the start of the λ monomer and dimer LD curves. Such an overshoot is not visible in the 5- or 10-bead chains of Figure 7B because this model uses 1-μm tube segments, and these tube segments make a poor random coil shape (zero-field case) for molecules whose normal end-to-end distances are only about 1 μm.

There is perhaps an upper limit to the molecular size that can be treated successfully because the model fails to reproduce the permanent immobilization of DNA molecules longer than 900 kbp in strong steady electric fields (Turmel et al., 1990b). This trapping occurs with increasing DNA size or increasing field strength. It is noticed in the simulation that molecules of any size form narrow U shapes that open downfield and have a sharp turning point. It has been proposed that DNA might get stuck at a turning point due to friction (Deutsch, 1987). If the U is symmetrical and the arms are long, then the static friction would be high at a sharp turning point. The higher the field, the sharper the turn by the action of eq 4. Accounting for static friction might improve the FIGE results where mobility minima are not wide enough at long pulse time, i.e., for molecules larger than 500 kbp in Figure 6A. The place where they lack width is on the high molecular weight side. Mobility minima are caused by temporary trapping in U shapes, and the static friction would prevent slipping off until a certain asymmetry was achieved in the U shape. We have not yet simulated static friction but it should not be difficult to implement in this type of model.

It is reasonable to expect the model to fail at very low electric field strengths (<1 V/cm) since the model makes no barrier whatever to the formation of a double-over kink other than requiring a local bunching of the chain. It is known, however, that there exist entropic and bending energy costs associated with forming such a kink inside a narrow tube or pore. The model assumes that these costs are negligible over the applicable range of conditions. While kinks certainly do form in high fields, it seems reasonable that kinks would fail to form when the field strength is below some critical value. In the simulations, however, if a chain is initialized as stretched ($s > 0.5$) and then allowed to relax in zero field, it will contract rapidly to its minimum bead spacing ($s = 0.12$) and then, due to the simulated Brownian forces, it may retract further from both ends by forming kinks in its middle. This second stage of contraction proceeds more slowly, requiring several thousand simulated seconds for a 50-bead chain. Our model's behavior would seem to violate statistical mechanics if the bending and entropic energy barriers much exceed $kT$. Real DNA in agarose exhibits a similar behavior, however. A long (500 kbp) stretched molecule in 1% agarose will usually contract rapidly from both ends but then contract slowly, over several thousand seconds, while forming globs or branches in its middle (Figure 3 of Smith et al., 1989; unpublished data). The reason that the energy barriers are not very large is that the kinks do not form inside small branching pores but rather inside large intervening "lakes". These lakes, often 1 μm in diameter, become evident in the microscope only after the molecule has contracted and the lakes have become filled with stained DNA. Smaller lakes are probably the nucleation points for kink formation in high fields as well. Given enough time and chain length, there seems to be no lower limit to the field required to form such a lake or globular kink. The fact that our model behaves similarly to experiment for contraction in zero field is mostly a coincidence, since no use is made of a pore size distribution (or even an average) in the model. A model like Zimm's "lakes and straights" (Zimm, 1988) should work best to explain DNA motion through agarose in very low fields.

A more obvious failing of the model is apparent from Figure 4, where the velocity of a simulated molecule is not a strong enough function of the field strength. The velocity is correct at 5 V/cm but not for lower or higher field strengths. The indirection of tube segments as a function of field strength,

as described by eq 4, causes the mobility (=velocity/field strength) to increase with field strength, but in the case of our simulation, the increase is not fast enough. Apparently the indirection of the submicroscopic zigzag path is itself a function of the electric field and subject to something like eq 4 but with a shorter lever arm and smaller charge. Changing maxBeadSpace (the parameter specifying the maximum bead spacing) with field strength could solve this problem if the component of the electrical force was then reduced by the factor maxBeadSpace/contourLength, as was done to the elastic force. For the case where the field strength changes during the experiment, as in zero integrated field electrophoresis (ZIFE) (Turmel et al., 1990a), each tube segment would have to be assigned its own maxBeadSpace as it was created, depending on the field strength that existed at the time of its creation. The need to adjust maxBeadSpace with field strength is further indicated by the observation that the reduced LD for T2 DNA in a steady field increases with field strength to a value of 0.6 at 45 V/cm [Figure 9 in Akerman et al. (1989)]. Assuming that the molecule is perfectly aligned with the field and each bead is spaced by the maxBeadSpace, eq 9 will give a value of 0.6 only if maxBeadSpace is increased to 2.8 $\mu$m, making $s = 0.82$.

Despite its limitations, the computer simulation is close enough to real experimental behavior to be useful as a research tool. To the extent that the simulation reproduces some mobility trait observed in real PFGE, the simulation can also display the individual molecular motions responsible for that trait.

This computer program is available free to anyone for the purpose of education or research. The version available from S. Smith runs on any IBM PC/XT/AT or compatible system with color monitor and 1 Mbyte memory. The source code and a compiled version will be sent on a 1.2-Mbyte 5.5-in. floppy disc. Also included is a time-lapse demonstration of previous simulations. To change the source code and recompile will require Borland's Turbo Pascal 4.0 or higher. With a 10-MHz computer clock rate, the simulated time and computation time are roughly the same when moving a 10-bead chain. For other lengths, computation time is proportional to the number of beads. To reproduce the data shown in Figure 6A,C (20 chains × 20 sizes averaging 50 beads for 5 pulse times and 1000 simulated seconds) would require 4 months of computation time on such a personal computer. A standard Pascal code for mainframe computers is available from C. Heller. The data summarized in Figure 6A,C were actually produced with this code and required 1 week of CPU time on a Comparex computer running under VM/CMS.

## Acknowledgments

We thank Fabio Biscarini for the basic idea leading to eq 8, Joerg Vreeman for help translating the program into standard Pascal, and Sergio Gurrieri for his help observing single-molecule relaxations.

## Appendix A

It is evident from Figure 5B that, for smaller DNAs such as λ monomers, the velocities asymptotically approach a value of 0.33 cm/h if the switch time is large (>5 s). This implies that the reorientation time is negligible for long switch times. For long switch times, the paths of λ monomers are ±60° zigzags and their speeds are essentially the same as their steady-field velocities at whatever field strength the PACE box produces. Accounting for the indirection of their paths (cos 60° = $^1/_2$), the λ monomers apparently have a steady-field velocity of 0.66 cm/h at the field strength used. We have measured the steady-field velocity of λ monomers in SeaKem ME agarose and 0.5× TBE buffer at 13 °C and found it to be 0.92 cm/h with 6 V/cm and 0.65 cm/h with 5 V/cm. Therefore, we have used a simulated field strength of 5 V/cm for the experiment of Figure 5, which nearly reproduces the steady-state speed of 0.66 cm/h in the PACE experiment. The PACE experiment actually used SeaKem LE agarose, which gives even greater steady-field velocities than ME agarose, i.e., 1.02 cm/h at 6 V/cm and 0.78 cm/h at 5 V/cm. This implies that the field strength which existed inside the PACE box was actually less than 5 V/cm. It is possible that our gels or buffers differ from those of Birren et al. (1988), but an important difference is the method for measuring the field strength. In our experiments, we insert platinum probe electrodes spaced at 10 cm into the buffer and measure the voltage drop with a high-impedance voltmeter. The method used by Birren et al. (1988) was to measure the voltage on the current delivering electrodes of the PACE array and divide by the distance across the hexagon. This method will overestimate the field strength near the center of the hexagon. The potential gradient increases near the wire driver electrodes because the current converges to a small radius there and because gas bubbles evolve from the wires and partially insulate them. The best way to test the electric field strength in a PACE apparatus would be to use separate probe electrodes that sink no current and that are rotated to give the maximum reading. This would also give a check on the angle through which the electric field tacks.

## Appendix B

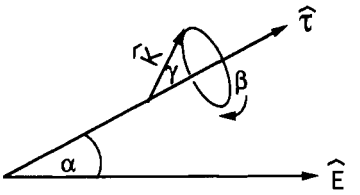


$\hat{E}$ is the polarization direction of the light, $\hat{\tau}$ is the direction of tension in the molecule, $\hat{K}$ is the direction of the Kuhn segment, $\alpha$ is the angle between $\hat{E}$ and $\hat{\tau}$, $\beta$ is a rotation of 0–2$\pi$ around $\hat{\tau}$, and $\gamma$ is the angle between $\hat{K}$ and $\hat{\tau}$. Define $\theta$ as the angle between $\hat{K}$ and $\hat{E}$. Select Cartesian coordinates such that

$$\hat{E} = \begin{bmatrix} 0 \\ 1 \\ 0 \end{bmatrix}$$

then

$$\hat{K} = \begin{bmatrix} \cos\beta \sin\alpha \cos\gamma \\ +\cos\alpha \sin\gamma \\ -\cos\beta \sin\alpha \sin\gamma \\ +\cos\alpha \cos\gamma \\ \sin\beta \sin\alpha \end{bmatrix}$$

from Euler angle transformations and

$$\cos\theta = \hat{E}\cdot\hat{K} = \cos\beta \sin\alpha \sin\gamma + \cos\alpha \cos\gamma$$

$$\sin^2\theta = 1 - \cos^2\theta = 1 - (-\cos\beta \sin\alpha \sin\gamma + \cos\alpha \cos\gamma)^2$$

Taking the thermal average of $\sin^2\theta$ gives

$$\langle\sin^2\theta\rangle = \left[\int_0^{\pi}\int_0^{2\pi}[1 - (\cos\alpha \cos\gamma - \cos\beta \sin\alpha \sin\gamma)^2]\, d\beta\; e^{-a\cos\gamma} \sin\gamma\, d\gamma\right] \Big/ \left[\int_0^{\pi}\int_0^{2\pi} d\beta\, e^{-(a\cos\gamma)} \sin\gamma\, d\gamma\right]$$

where $a = b\tau/kT$, $b$ is the Kuhn length, $\tau$ is the tension in the chain, and $kT$ is the thermal energy.

The inner integral reduces to

$$2\pi(1 - \cos^2\alpha \cos^2\gamma - \tfrac{1}{2} \sin^2\alpha \sin^2\gamma)$$

so

$$\langle \sin^2\theta \rangle = \left[2\pi \int_0^\pi (1 - \cos^2 \cos^2\gamma - \tfrac{1}{2} \sin^2\alpha \sin^2\gamma) e^{-(a \cos\gamma)} \sin \gamma \, d\gamma\right] \Big/ \left[2\pi \int_0^\pi e^{-(a \cos \gamma)} \sin \gamma \, d\gamma\right]$$

Substitute $X = \cos \gamma$ and $dx = -\sin \gamma \, d\gamma$:

$$\langle \sin^2\theta \rangle = 1 - \frac{\cos^2\alpha \int_{-1}^{1} x^2 e^{-ax} \, dx}{\int_{-1}^{1} e^{-ax} \, dx} - \frac{\sin^2 \alpha \int_{-1}^{1} (1 - x^2) e^{-ax} \, dx}{2 \int_{-1}^{1} e^{-ax} \, dx}$$

Note that

$$\int_{-1}^{1} x^2 e^{-ax} \, dx = 1 - 2L(a)/a$$

where $L(a) = \coth a - 1/a$ is the Langevin function.

$$\langle \sin^2\theta \rangle = 1 - \cos^2\alpha \left[1 - \frac{2L(a)}{a}\right] - \frac{\sin^2\alpha}{2}\left[1 - \left(1 - \frac{2L(a)}{a}\right)\right]$$

$$\langle \sin^2\theta \rangle = \sin^2 \alpha \left(1 - \frac{3L(a)}{a}\right) + \frac{2L(a)}{a}$$

Substitute $s = L(a)$ and $a = L^{-1}(s)$, where $s$ is the fractional elongation of the chain or the end–end distance/contour length:

$$\langle \sin^2\theta \rangle = \sin^2 \alpha \left(1 - 3\frac{s}{L^{-1}(s)}\right) + 2\frac{s}{L^{-1}(s)}$$

A more general treatment is found in Flory (1969).

## References


Akerman, B., Jonsson, M., & Norden, B. (1989) *Biopolymers 28*, 1541.

Birren, B. W., Lai, E., Clark, S. M., Hood, S., & Simon, S. I. (1988) *Nucleic Acids Res. 16*, 7563.

Bueche, F. (1962) *Physical Properties of Polymers*, p 37, Interscience, New York.

Carle, G. F., Frank, M., & Olson, M. V. (1986) *Science 232*, 65.

deGennes, P. G. (1971) *J. Chem. Phys. 55*, 572.

Deutsch, J. M. (1987) *Phys. Rev. Lett. 59*, 1255.

Deutsch, J. M. (1988) *Science 240*, 922.

Deutsch, J. M. (1989) *J. Chem. Phys. 90*, 7436.

Deutsch, J. M., & Madden, T. L. (1989) *J. Chem. Phys. 90*, 2476.

Duke, T. A. J. (1989) *Phys. Rev. Lett. 62*, 2877.

Flory, P. J. (1969) *Statistical Mechanics*, Chapter 9, Wiley, New York.

Gurrieri, S., Rizzarelli, E., Beach, D., & Bustamante, C. (1990) *Biochemistry 29*, 3396.

Heller, C. (1990) Ph.D. Dissertation, Universität Konstanz, Konstanz, FRG.

Heller, C., & Pohl, F. M. (1989) *Nucleic Acids Res. 17*, 5989.

Holzwarth, G., McKee, C. B., Steiger, S., & Crater, G. (1987) *Biopolymers 15*, 10031.

Lerman, L. S., & Frisch, H. L. (1982) *Biopolymers 21*, 995.

Lim, H. A., Slater, G., & Noolandi, J. (1990) *J. Chem. Phys. 92*, 709.

Lumpkin, O. J., & Zimm, B. H. (1982) *Biopolymers 21*, 2315.

Lumpkin, O. J., Dejardin, P., & Zimm, B. H. (1985) *Biopolymers 24*, 1575.

Manning, G. R. (1978) *Q. Rev. Biophys. 11*, 179.

Olson, M. V. (1989) in *Genetic Engineering* (Setlow, J. K., & Hollaender, A., Eds.) Vol. 11, p 183, Plenum Press, New York.

Olivera, B. M., Baine, P., & Davidson, N. (1964) *Biopolymers 2*, 245.

Olvera de la Cruz, M., Deutsch, J. M., & Edwards, S. F. (1986) *Phys. Rev. A 33*, 2047.

Olvera de la Cruz, M., Gersappe, D., & Shaffer, E. O. (1990) *Phys. Rev. Lett. 64*, 2324.

Schwartz, D. C., & Cantor, C. R. (1984) *Cell 37*, 67.

Schwartz, D. C., & Koval, M. (1989) *Nature 338*, 520.

Slater, G. W., & Noolandi, J. (1985) *Biopolymers 24*, 2181.

Smith, S. B., & Bendich, A. J. (1990) *Biopolymers 29*, 1167.

Smith, S. B., Aldridge, P. K., & Callis, J. B. (1989) *Science 243*, 203.

Southern, E. M., Anand, R., Brown, W. R. A., & Fletcher, D. S. (1987) *Nucleic Acids Res. 15*, 5925.

Turmel, C., Brassard, E., Forsyth, R., Hood, K., Slater, G. W., & Noolandi, J. (1990a) in *Current Comments in Cell & Molecular Biology: Electrophoresis of Large DNA Molecules; Theory & Applications* (Birren, B., & Lai, E., Eds.) Cold Spring Harbor Press, Cold Spring Harbor, NY.

Turmel, C., Brassard, E., Slater, G. W., & Noolandi, J., (1990b) *Nucleic Acids Res. 18*, 569.

Yanagida, M., Hiraoka, Y., & Katsura, I. (1963) *Cold Spring Harbor Symp. Quant. Biol. 47*, 177.

Zimm, B. H. (1988) *Phys. Rev. Lett. 61*, 2965.